DOI: 10.1070/RCR4859

Graphene – quantum dot hybrid nanostructures with controlled optical and photoelectric properties for solar cell applications

Pavel M. Sokolov,[a] Maria A. Zvaigzne,[a] Victor A. Krivenkov,[a] Alexander P. Litvin,[b] Alexander V. Baranov,[b] Anatoly V. Fedorov,[b] Pavel S. Samokhvalov,[a] Igor R. Nabiev [a, c]

[a] National Research Nuclear University MEPhI (Moscow Engineering Physics Institute)
Kashirskoe shosse 31, 115409 Moscow, Russian Federation
[b] Saint Petersburg National Research University of Information Technologies, Mechanics and Optics (ITMO University)
Kronverksky prosp. 49, 197101 Saint Petersburg, Russian Federation
[c] University of Reims Champagne-Ardenne (URCA)
51 str. Cognacq Jay, 51100 Reims, France

State-of-the-art research related to increasing the efficiency and reducing the cost of solar energy converters is analyzed. An approach to solving these issues is to introduce graphene and its derivatives into the photoactive layer of solar cells. These materials have record high charge carrier mobility at normal temperatures and low absorption cross-sections of solar radiation. The review considers chemical materials science methods and nanotechnology approaches to the design of 2D hybrid structures based on graphene and quantum dots. Examples of their most successful use in solar cells are given and promising areas of research and development in this field are formulated.
The bibliography includes 173 references.

Contents

1. Introduction 370
2. Modern types of solar cells 371
3. Two-dimensional graphene – quantum dot hybrid structures. The synthesis and properties of individual components and prerequisites for their use in solar cells 375
4. Solar cells based on 2D graphene – quantum dot hybrid structures 377
5. Conclusion 382

1. Introduction

Solar radiation is a non-exhaustive source of energy. The amount of solar energy absorbed by the Earth's atmosphere every hour exceeds that the human civilization uses every year.[1] The yearly solar energy production increased from 31.4 to 253 TWh (*i.e.*, by a factor of about 8) between 2010 and 2015, thus demonstrating the highest growth rate

P.M.Sokolov. Candidate of Biological Sciences, Engineer, NRNU MEPhI.
Telephone: +7(495)788 – 5699 (ext. 8088), e-mail: socolovpm87@mail.ru
M.A.Zvaigzne. Engineer, Post-graduate Student, NRNU MEPhI.
Telephone: +7(495)788 – 5699 (ext. 8088),
e-mail: mariazvaigzne@gmail.com
V.A.Krivenkov. Candidate of Physical and Mathematical Sciences, Junior Researcher, NRNU MEPhI.
Telephone: +7(495)788 – 5699 (ext. 8088), e-mail: vkrivenkov@list.ru
A.P.Litvin. Candidate of Physical and Mathematical Sciences, Researcher, ITMO University.
Telephone: +7(812)232 – 9704, e-mail: litvin@niuitmo.ru
A.V.Baranov. Doctor of Physical and Mathematical Sciences, Professor, ITMO University.
Telephone: +7(812)232 – 9704, e-mail: a_v_baranov@yahoo.com
A.V.Fedorov. Doctor of Physical and Mathematical Sciences, Professor, ITMO University.
Telephone: +7(812)232 – 9704, e-mail: a_v_fedorov@inbox.ru
P.S.Samokhvalov. Candidate of Chemical Sciences, Senior Researcher, NRNU MEPhI.
Telephone: +7(495)788 – 5699 (ext. 8088),
e-mail: p.samokhvalov@gmail.com
I.R.Nabiev. Doctor of Chemical Sciences, Leading Scientist in the Laboratory of Nano-Bioengineering, NRNU MEPhI; Head of Laboratory of Research in Nanosciences, Director of European Technological Plateform 'Semiconductor Nanocrystals' and Professor at URCA.
Telephone: +33(0)326 – 918127, e-mail: igor.nabiev@univ-reims.fr
Current research interests of the authors: nano- and biotechnologies, chemical synthesis, photovoltaics.

Received 31 August 2018
Translation: A.M.Raevskiy

© 2019 Uspekhi Khimii, Russian Academy of Sciences and Turpion Ltd.

compared to other alternative energy sources; in the last decade, the solar energy production showed a 70-fold increase.[2] Despite this fact, solar energy accounts for only 1% of total energy production.[2]

The photovoltaic effect was for the first time demonstrated in 1839 and the first solar array with an efficiency of merely 1% was installed on a rooftop in New York (USA) in 1884. Intensive development and introduction of solar cell technologies began in almost a century when the problem was posed of search for energy sources that represent an alternative to natural fossil fuels (petroleum, gas and coal). The energy conversion efficiency (ECE) of modern commercially available solar cells is about 25%, being as high as 46% for the best laboratory-scale samples of different-type cells.[3]

The last decade was marked by the introduction of nanotechnologies into many areas of science, and the results of such studies are successfully used in practice. In particular, candidate nanostructures for photovoltaics applications include graphene and semiconductor quantum dots (QD).† Graphene is a one atom thick 2D carbon structure having record high charge carrier mobility and unique electrophysical properties as compared to other 2D structures.[4] Quantum dots are inorganic semiconductor nanocrystals. They are smaller than the exciton Bohr radius for the bulk materials and exhibit pronounced quantum size effects. This allows one to change the absorption and luminescence spectra of QDs by choosing appropriate materials and by varying the QD size.

Combining various QD materials and QD size makes it possible to extend the spectral range of efficient absorption of solar radiation.[5] A unique feature of QDs is the possibility to generate more than one exciton (electron – hole pair) upon absorption of a single photon, which allows one to achieve a quantum efficiency exceeding 100%.[6] The development of cheap methods for the synthesis of graphene, which possesses unique electrical and optical properties, opened the way to solar cell applications of this material. Graphene – QD combination has been a basis for a new type of stable and rather efficient solar cells. The need for the development of solar cells based on nanostructures cannot be understood to the full extent without a brief survey of the existing types, stability, reliability, efficiency and production cost of these devices.

Depending on the fabrication technology and materials used, there are three generations of solar cells:[7]

— first-generation cells are based on single-crystalline (c-Si) or polycrystalline (poly-Si) silicon or gallium arsenide (GaAs) wafers;

— second-generation, or thin-film, cells are fabricated from amorphous silicon (a-Si:H), cadmium telluride (CdTe) or copper – indium – gallium selenide (CIGS);

— third-generation cells are made of advanced materials including dyes and other organic compounds, quantum dots, perovskites; exotic concepts like multijunction cells, 'hot-carrier' cells, *etc*. are also used.[8]

Besides, there are solar cells that combine thin films of various semiconductors; this provides efficient absorption of solar energy in different spectral regions. Although such systems represent a particular case of second-generation devices, they are sometimes treated as a specific class of solar cells.[9]

The US National Renewable Energy Laboratory (NREL) publishes the best photovoltaics efficiency charts and carries out a retrospective analysis of increasing their efficiency depending on the cell generation and type. Figure 1 presents the solar cell efficiency data for a period since 1976. Shown are the dynamics of changes in the cell efficiency; the key factors, discoveries and innovations that made the greatest contribution to these dynamics are also specified.[10]

In this review we briefly outline various types of solar cells and trends in their development. Factors underlying the design of solar energy converters using graphene and quantum dots and 2D hybrid nanostructures based on them will be considered in detail. The synthesis of such nanomaterials and the properties of graphene and quantum dots will be discussed.

The fabrication technology of graphene – QD cells has been developed for about a decade. There are a number of reviews on utilization of graphene in different types of solar cells, *e.g*., publications by Martinez-Ferrero[11] and Kymakis[12] as well as studies on the design of QD-based solar cells reported by Yamaguchi,[13] Sargent[14] and Beard.[15] However, no feature publications on the application of graphene – QD hybrid nanostructures and fabrication of solar cells based on them are available as yet. The authors of this review tried to bridge the gap, to collect actual information, to help to structure the available knowledge and to formulate the issues to be solved in the future.

Notations are as follows:

Cl-GO — chlorinated graphene oxide,
ECE — energy conversion efficiency,
EDT — ethane-1,2-dithiol,
EIL — electron injection layer,
FTO — fluorine doped tin oxide,
HIL — hole injection layer,
HOMO — highest occupied molecular orbital,
ITO — indium – tin oxide,
LUMO — lowest unoccupied molecular orbital,
PEDOT:PEG — poly(3,4-ethylenedioxythiophene) polyethylene glycol,
PEDOT:PSS — poly(3,4-ethylenedioxythiophene) polystyrene sulfonate,
TBAI — tetrabutylammonium iodide,
RGO — reduced graphene oxide,
QDs — quantum dots,
V_{oc} — open-circuit voltage.

2. Modern types of solar cells

2.1. First-generation solar cells

First-generation solar cells account for about 90% of the cells produced so far. They can be fabricated from both single-crystalline and polycrystalline silicon and from gallium arsenide.

A typical structure of a first-generation solar cell is shown in Fig. 2. The cell comprises an optically transparent photoanode coated on a glass substrate, doped crystalline n-Si and p-Si wafers and a photocathode that is most often optically opaque. Conventional dopants include boron and arsenic. Thus, the junction points of the doped silicon wafers represent p – n junctions where charge separation occurs.[16]

† See, *e.g*., a review by L.M.Nikolenko, V.F.Razumov 'Colloidal quantum dots in solar cell'. *Russ. Chem. Rev*. **82**, 429 (2013).

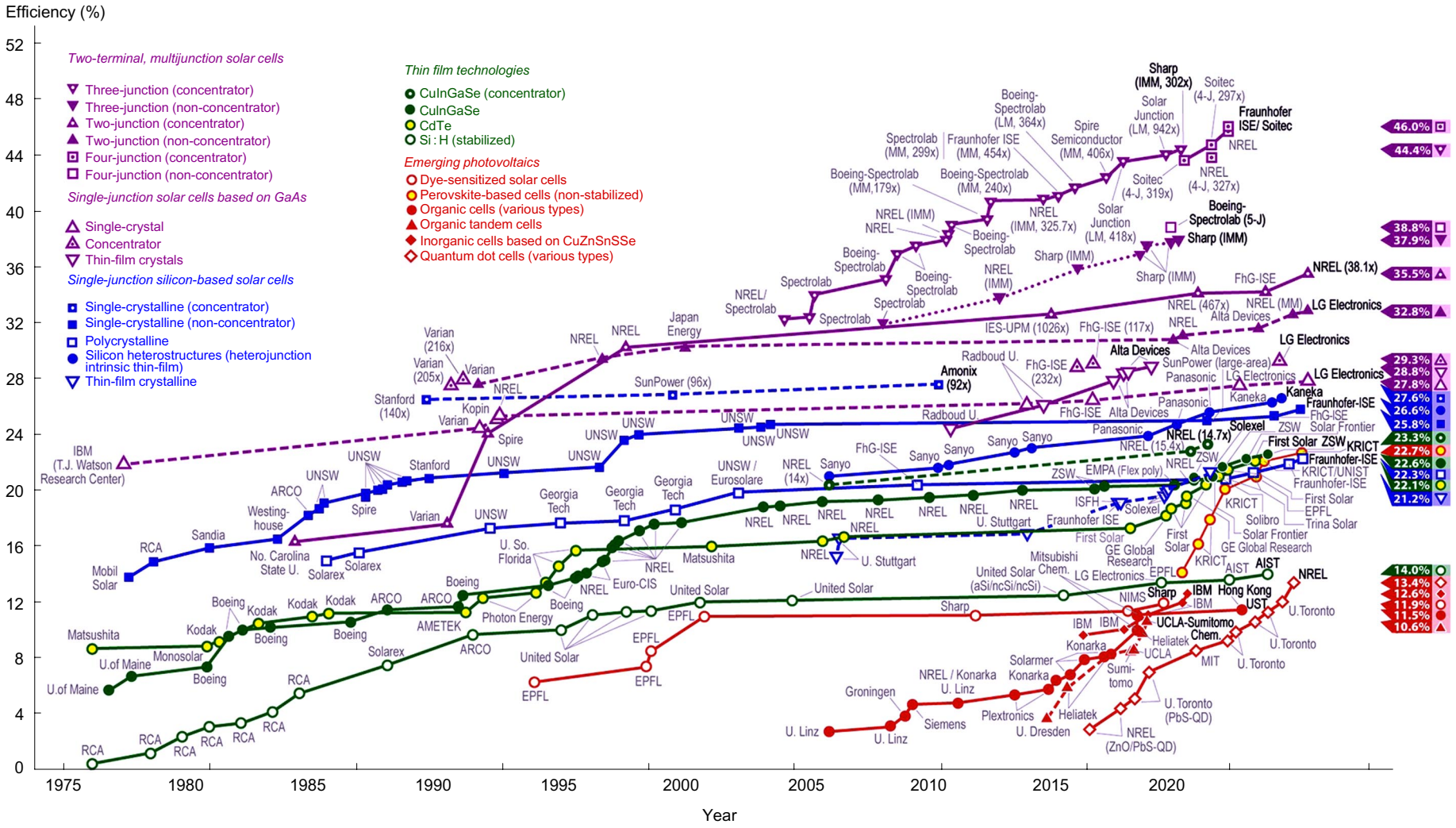


Figure 1. Best cell efficiencies for various types of solar cells fabricated by leading manufacturers.[10] Solar cell types: LM is lattice matched, MM is metamorphic, IMM is inverted metamorphic; U. stands for University.

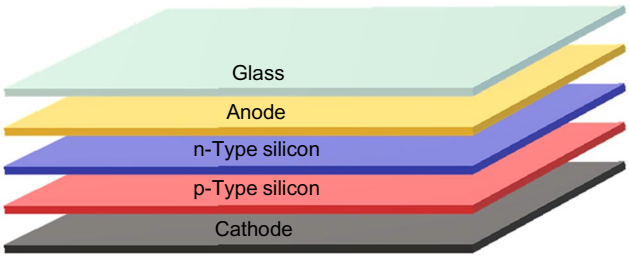


Figure 2. Structure of a first-generation solar cell.

The efficiency of solar cells based on single- and polycrystalline Si reaches a value of 26.1% and 22.3%, respectively.[17] Silicon accounts for nearly 50% of the total cost of the system. Since single-crystalline silicon is much more expensive than polycrystalline silicon, cells based on the former are much more costly than those based on the latter. First-generation cells are characterized by stable operation, but their efficiency decreases at high temperatures and under mechanical load.[18]

2.2. Second-generation solar cells

In second-generation solar cells (or thin-film solar cells), semiconductor (amorphous and microcrystalline silicon, cadmium telluride or cadmium sulfide, *etc.*), thin films 10–100 nm thick are coated on glass, metallic or plastic substrates. Thin layers of photovoltaic compounds are separated by relatively thick silicon layer (250–500 nm thick) called the intrinsic layer. As a result, a p–i–n junction is formed. The intrinsic layer provides an increase in the light absorption range and allows a larger number of excitons to separate into free charge carriers; as a consequence, the short-circuit current increases. The structure of a thin-film solar cell with two p–i–n junctions and two intrinsic layers (a-Si layer and a-Si/Ge alloy layer) is shown in Fig. 3.

Solar cells with multiple p–i–n junctions enable efficient absorption of the Sun light at several different wavelengths. Modern cells with, *e.g.*, three p–i–n junctions can be fabricated. For instance, the initial efficiency of a structure composed of doped a-Si, a Si/Ge alloy and microcrystalline silicon (here, the crystalline phase is incorporated into the amorphous matrix) was as high as 13.4%.[19] Besides, doping the a-Si intrinsic layer with boron to a concentration of 0.1–1 ppm provides a more efficient separation of charge carriers owing to generation of additional electric field.[20] Solar cells based on silicon heterostructures comprising a single-crystalline silicon wafer a few hundred micrometres thick sandwiched between ultrathin layers of doped a-Si with n- and p-type conductivity are available.[21] They are produced by the microelectronics market leaders, *e.g.*, Panasonic Corp. and Sanyo Electric Co., Ltd. (both companies from Japan). In the Russian Federation this type of solar cells is developed at Hevel Group in collaboration with the Ioffe Physical-Technical Institute of the Russian Academy of Sciences. To date, Hevel Group has been among the world leaders in production of heterostructure solar cells with an efficiency of 22.6%–22.8%.[22]

A more complicated structure composed of $Cu(InGa)Se_2$ as p-layer, the CdS intrinsic layer, and ZnO as n-layer instead of differently doped a-Si layers is characterized by an ECE of 21.7%.[23]

Thin-film solar cells based on CdTe form a particular group. Cadmium telluride is a readily available, stable, direct-band-gap semiconductor with a band gap of 1.49 eV and a high light absorbance; it is promising for fabrication of thin-film solar cells.[24] This compound is used to fabricate systems with transparent electrodes that transmit up to 85% of solar energy and an efficiency of more than 22%.[20]

The proportion of thin-film solar cells based on a-Si and $Cu(InGa)Se_2$, respectively, decreased from 8% to 1% and from 3% to 2% between 2010 and 2014, whereas the cells based on CdTe showed an increase from 3% to 5%.[25] Undoubtful advantages of thin-film solar cells include low production cost, mechanical stability and the possibility to fabricate transparent solar cells.

2.3. Third-generation solar cells

Third-generation solar cells are based on complicated hybrid structures fabricated using organic dyes and other organic polymers (dye-sensitized solar cells), QDs (organic photovoltaic cells) and perovskites. A salient feature of this type of cells is that no bulk crystalline materials are used. This allows one to fabricate flexible solar cells of complex shape. The structures of various third-generation solar cells are schematically shown in Fig. 4.

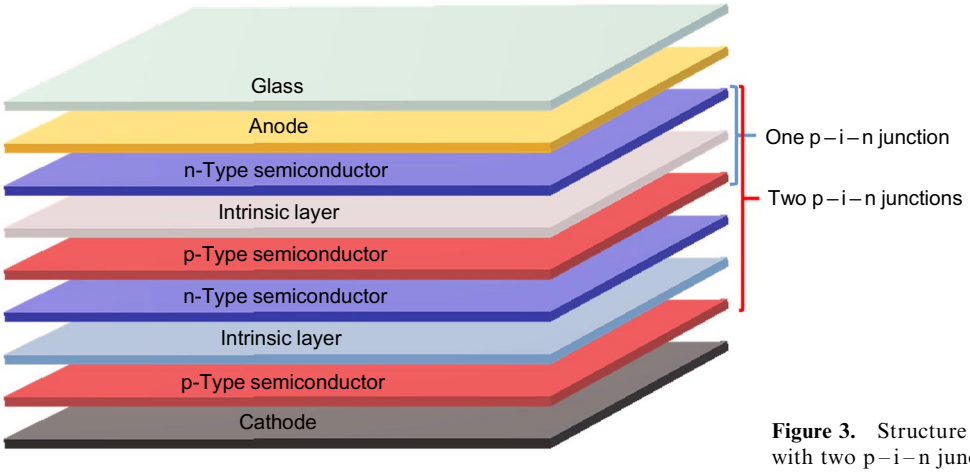


Figure 3. Structure of a thin-film solar cell with two p–i–n junctions.

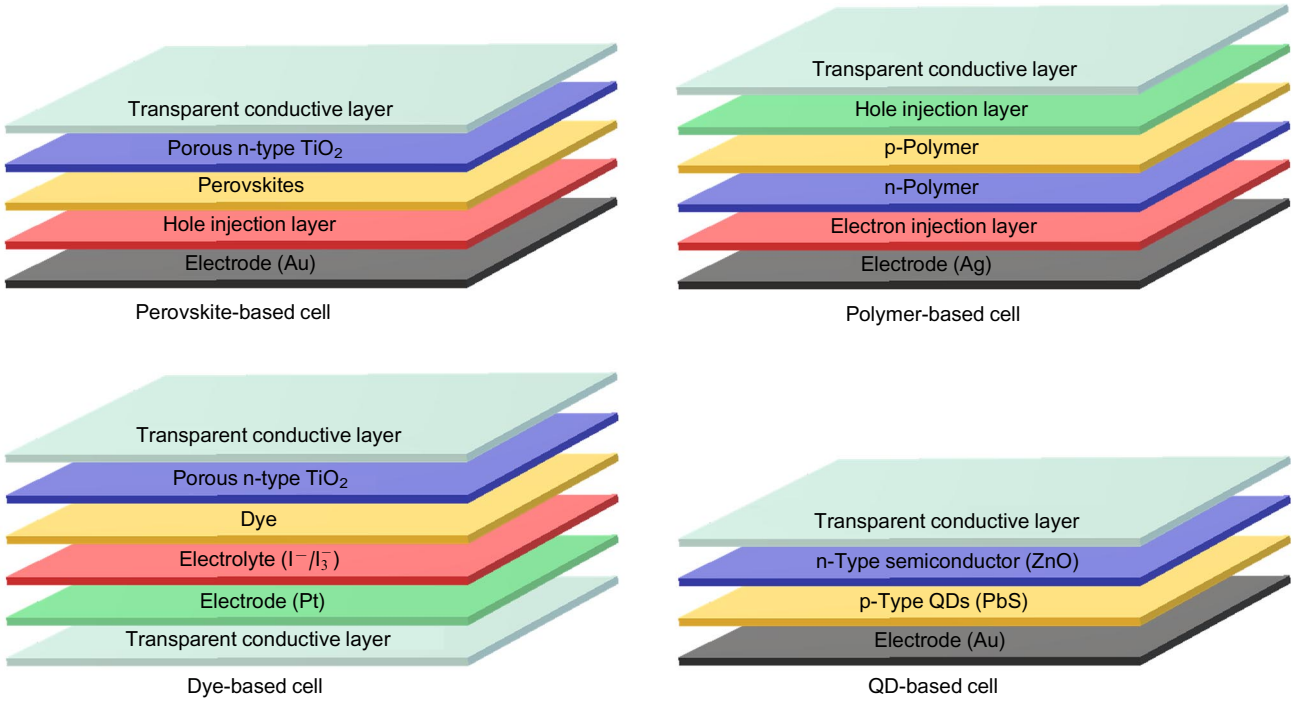


Figure 4. Structures of third-generation solar cells.

Usually, anodes of dye-sensitized solar cells (DSSC)‡ are coated with highly porous TiO_2 whose well-developed TiO_2 surface is covered with adsorbed dye molecules.[27] The operating principles, various electron transport processes, regeneration of oxidized dyes, as well as compounds, electrolytes, electrodes and the structure of DSSC were considered in a review by Hagfeldt *et al.*[28]

Often, high-performance multiple-junction solar cells utilize fullerene derivatives as electron acceptors[29] due to unique symmetrical 3D fullerene structure. However, high cost of fullerenes as well as insufficiently high stability and low absorption of sun radiation in the UV region gave an impetus to the search for alternatives to fullerenes. Research activity in this field was analyzed in a review by Wadsworth *et al.*[30] Considerable disadvantages of the cells based on fullerene derivatives include low thermal and radiation stability[31] as well as high cost since these materials are traditionally synthesized using expensive metals (platinum and ruthenium).[32]

Perovskites are compounds isostructural to the mineral perovskite $CaTiO_3$. They can act as solar energy converters into electricity. Although this property of perovskites was discovered quite recently,[33] perovskite solar cells (PSCs) demonstrate rather high ECE. Practically used films are about 0.5 μm thick.[34, 35] The perovskite materials ABX_3 are composed of a monovalent cation [$A = CH_3NH_3^+$, $CH(NH_2)_2^+$, Cs^+], a divalent metal cation ($B = Pb^{2+}$, Sn^{2+}), and halide anions ($X = Br^-$, I^-).[36, 37] Perovskite films are characterized by a narrow band gap, good light absorbance, long mean free paths of charge carriers and low probability of recombination.[38] To improve the ECE, perovskites are often coated on porous TiO_2 or on TiO_2 nanotubes. Solar cells comprising perovskite thin films sandwiched between injection layers were also reported. Cheap materials for and rather simple technology of fabrication of PSCs make this type of devices commercially competitive,[39] while high ECE and the possibility to vary the band gap over a wide range make them a good alternative to the widely used Si-based solar cells.[40] However, PSCs are moisture sensitive[41] and contain toxic lead.[42]

Organic polymer solar cells can be one- and two-layer and mixed type. One-layer systems contain an organic polymer sandwiched between two electrodes with high and low work function. Absorption of light causes the formation of excitons in the polymer layer and subsequent dissociation of these quasi-particles into electrons and holes under the action of electrode potentials. Two-layer cells contain two different polymer layers, that is, a donor layer and an acceptor layer. This structure provides more efficient charge separation than one-layer cells.

In mixed-type organic solar cells the role of electron donors is played by conjugated polymers, while fullerenes act as electron acceptors.[43] To improve the efficiency of this type of systems, one should extract photogenerated charge carriers from the active layer. This can be done using the so-called electron and hole injection layers (EIL and HIL) for the negative and positive charge carriers, respectively.[44] Disadvantages of this type of solar cells include low stability (due to high sensitivity to oxidation) and low light absorbance.

Solar cells based on QDs make use of the unique QD properties, namely, the dependence of the band gap on the QD size and high efficiency of absorption of solar radiation in the visible and near-IR regions.[45] This allows one to fabricate multiple-junction cells using QDs of identical composition but different size.[46] There has been consider-

‡ These cells are also called dye-sensitized Grätzel cells by the name of the author of a breakthrough research article published in *Nature* in 1991.[26]

able R&D activity on QD-based cells. Their ECE reached a value of 9.2% by the year 2015,[47] 10.4% in the beginning of 2017 (Ref. 48) and a record high value of 13.4% by October, 2017.[49] Undoubtful advantages of QD-based solar cells include high stability and light absorbance. However, the efficiency of charge transport is low and depends on the quality of the QD layer and on the surface ligands used.[50]

The best cell efficiencies for various types of solar cells (see above) obtained in different years are collected in Table 1. Recently, these values significantly changed. An important factor that markedly affected the efficiency of third-generation solar cells is the use of graphene, a 2D material representing a single layer of carbon atoms arranged in a hexagonal lattice. Graphene is characterized by record high charge carrier mobility; this makes possible efficient extraction of charge carriers from QDs and transport within the photoactive layer. When the EIL and HIL contain graphene, the energy barriers to charge transfer from the photosensitive units to electrodes decrease and directed charge transport becomes possible. Low light absorbance of graphene allows the total luminous flux to be used by the photosensitive units. Besides, graphene and its derivatives, *e.g.*, graphene oxide (GO), RGO as well as graphene complexes with various compounds are used as transparent, flexible, efficient and stable electrodes.[53, 54]

Table 1. Best cell efficiencies for various types of solar cells.

Classification	Year	Efficiency (%)	Ref.
QDs	2017	13.4	49
Organic polymers	2018	14.2	51
Dyes	2011	11.9	52
Perovskites	2018	20.9	3
Perovskite/Si	2017	23.6	3

3. Two-dimensional graphene – quantum dot hybrid structures. The synthesis and properties of individual components and prerequisites for their use in solar cells

Quantum dots are semiconductor nanocrystals whose size varies from a few to several tens of nanometres. The luminescent properties, quantum yield and fluorescence brightness of QDs depend on their size, structure and composition. Quantum dots have a large absorption cross-section, can efficiently absorb solar radiation in a wide spectral range and transfer excitation nonradiatively by the Förster resonant energy transfer mechanism; therefore, they act as so-called nanoantennas for visible radiation and transfer it to other photosensitive components of hybrid materials[55] that are used in photocatalysis[56] and to fabricate solar cells.[57, 58]

Depending on the aggregation state of the reaction medium, solid-phase, liquid-phase and gas-phase methods for the synthesis of QDs are distinguished. However, the first and third methods have technological constraints and often cannot compete in product quality with the most widely used liquid-phase method.[59] Liquid-phase synthesis is carried out in aqueous or organic media and rarely at the interface between these two phases.[60] The synthesis in aqueous media immediately produces water-soluble QDs; however, nucleation of new QDs and growth of the available QD seeds compete with each other owing to low growth temperature in the reaction medium and thus preclude efficient control of QD morphology.[61] High-temperature aqueous synthesis of QDs under high pressures is also possible. This is the so-called hydrothermal synthesis that allows one to reduce the size of QDs produced but is inappropriate to significantly improve their optical properties.[62]

A version of the liquid-phase method is organometallic synthesis in high-boiling organic solvents, which affords size-homogeneous QDs and is characterized by good reproducibility of results,[63] high product yield and high QD concentrations;[64] this is of great importance for large-scale production of QD-based systems.

Quantum dots have a core that can be coated with outer epitaxial inorganic single- or multilayer shell. The core materials include silicon, carbon, graphene or compounds of Group III – V, II – VI or IV – VI elements; the shell improves the optical properties of QDs and their stability against environmental factors.[65, 66] It should be noted that core/shell QDs are characterized by weaker charge carrier recombination on core defects; besides, charge carriers can be confined within the core provided that the epitaxial shell is fabricated from wide-band-gap materials, such as ZnS or CdS.[67]

Surface ligands are of great importance from the standpoint of improving the stability and optical properties of QDs. Ligands are also needed to fabricate hybrids comprising QDs and other materials and to specify, along with the outer shell, the most probable paths of charge transfer and separation as well as charge carrier recombination in excited QDs.[68] Problems related to the synthesis of QDs and to the choice of certain types of ligands for fabrication of hybrid materials were considered in detail in reviews by Samokhvalov *et al.*[69] and by Zvaigzne *et al.*,[70] respectively.

Quantum dots used in modern solar cells can have cores composed of either heavy metals (CdTe, CdS, CdSe, PbS, ZnS)[71] or containing no heavy metals ($CuInS_2$, $CuInSe_2$).[72, 73] Core/shell QDs, *e.g.*, $AgInS_2$/ZnS (Ref. 74) and $CuInS_2$/Zn (Ref. 75) are also used. The theoretical ECE of QD-based cells can be as high as 44%, which is much higher than for other types of currently available solar cells. Considering efficient absorption of light in different spectral ranges, thin-film cells with multiple p – i – n junctions are required; in the case of QD-based cells, this can be done with ease by varying the QD size or composition. However, owing to (i) high probability of charge carrier recombination on the QD surface inhomogeneities and at interfaces with other components of the photoactive layer and (ii) recombination loss of electrons in the electrolyte, the ECE of real QD-based solar cells is nearly four times lower than the theoretical value.[76] The use of graphene and graphene derivatives will decrease this ratio.

Interest of researchers in graphene increased after publication by Novoselov *et al.*,[4] who described a simple method for preparation of the material by mechanical exfoliation of graphite onto a Scotch tape. However, early steps in the development of methods for the synthesis of graphene date back to the 1970s.[77] Graphene can be synthesized using two strategies called top down and bottom-up. Following the former approach, graphene is prepared from a bulk allotrope of carbon, *e.g.*, graphite, by mechanical or chemical exfoliation[78] or by dissolution.[79]

The other approach assumes the synthesis of graphene from carbon by, *e.g.*, epitaxial growth on a substrate,[80] chemical vapour deposition,[81] or reduction of carbon monoxide.[82] Each method has its own advantages and drawbacks. In particular, mechanical exfoliation is a simple method that allows one to prepare single-layer or few-layer graphene, but the reproducibility of the results is very low. The epitaxial growth technique makes it possible to obtain reproducible results; however, the problem is posed of graphene separation from the substrate. Reviews on methods for the synthesis of graphene with the description of key advances for each method were reported by Bhuyan *et al.*[83] and by Wang *et al.*[84]

Not only graphene, but also graphene derivatives are constituents of solar cells as well as systems for targeted drug delivery in living organisms, biosensors and many other products of modern nanotechnologies. Graphene can be modified in different manners, *viz.*,

— through covalent bonding, *i.e.*, with violation of the initial structure of the material due to, *e.g.*, doping with certain atoms or treatment of GO with surfactants, ionic liquids, chromophores, free radicals, *etc.*; or

— involving van der Waals forces, electrostatic interaction, formation of hydrogen or coordination bonds, as well as stacking.[85]

The modification strategy allows one to change the solubility of graphene by introducing hydrophobic or hydrophilic groups into the structure of the material,[86] to make it thermally or pH-sensitive,[87] to vary its mechanical properties by, *e.g.*, inducing the buildup of various 3D forms,[88] to change its electrical and photoelectrical properties[89] by reducing the resistance of polymers[90] or by increasing the absorption or fluorescence of other materials[91,92] in graphene-based composites and hybrid systems. Undoubtedly, the application field of graphene and graphene derivatives will extend in the future; however, this depends on how soon green technologies for production of commercially competitive high-quality graphene can emerge.[93]

The application of graphene in QD-based solar cells significantly improves the electron transport in the photoactive layer. The structure of a solar cell based on 2D graphene–QD hybrid structures is shown in Fig. 5.[94] Pio-

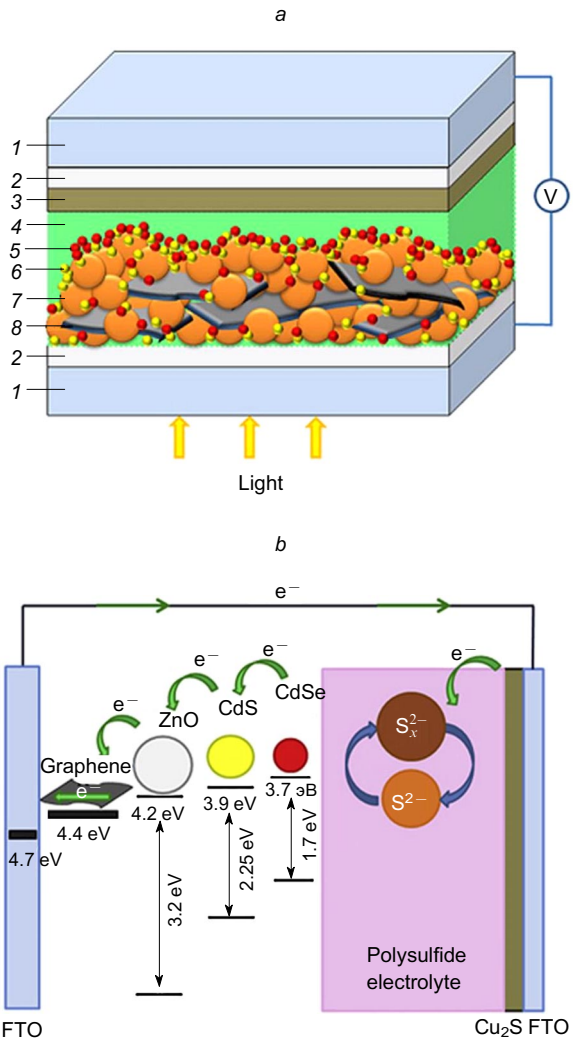


Figure 5. Graphene–QD hybrid cell (*a*) and the energy band diagram for the ZnO–graphene/CdS/CdSe structure (*b*).[94] Glass (*1*), FTO (*2*), Cu_2S (*3*), electrolyte (*4*), CdSe (QDs) (*5*), CdS (QDs) (*6*), ZnO nanoparticles (*7*) and graphene (*8*).

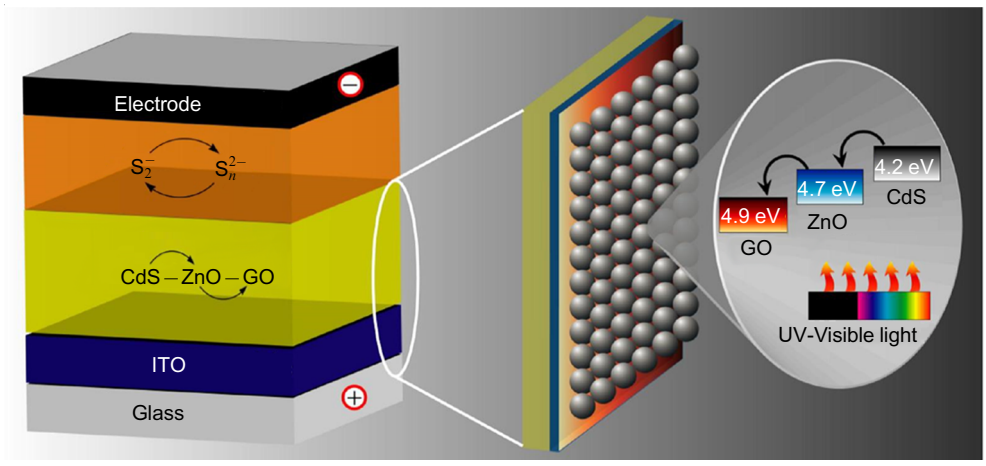


Figure 6. Structure of a ITO/ZnO–CdS–GO/Pt solar cell.[96] ITO is indium–tin oxide and GO is graphene oxide.

neering results in the field were reported by Guo *et al.*,[95] who fabricated a photoanode from graphene layers and CdS QDs. Graphene layers were electrophoretically deposited onto indium–tin oxide (ITO) glass while QDs were synthesized by sequential chemical deposition from corresponding aqueous solutions. Barpuzary *et al.*[96] described a solar cell (Fig. 6) with a ZnO–CdS QD–GO composite photoanode and an ECE of 2.82% achieved owing to favourable band-gap alignment. Zhu *et al.*[97] fabricated a solar cell where fluorine-doped tin oxide (FTO) glass was spin coated with a TiO_2-doped graphene layer and then the CdS and ZnS QDs were solution deposited on the surface of that layer; the ECE of this device was 4.2%. Kim *et al.*[98] reported a solar cell fabricated from multilayer stacks of PbS QDs and graphene, which made it possible to increase the ECE to 9.18%.

Graphene is an efficient medium for both transport and recombination of separated charge carriers. The mechanisms of charge carrier generation, separation and transfer, as well as the influence of the outer shell and QD ligands on these processes were considered in a review;[68] key problems related to charge carrier generation and recombination in graphene were analyzed elsewhere.[99, 100]

The aforesaid suggests that improvement of the structures of graphene-based solar cells should involve optimization of dopants, the QD and surface ligand compositions, methods for fabrication of 2D graphene–QD hybrid structures and criteria for the choice of auxiliary components.

4. Solar cells based on 2D graphene–quantum dot hybrid structures

Unique properties of QDs and graphene make 2D graphene–QD hybrid structures promising for fabrication of solar cells. Specific features of QDs are as follows:

— efficient absorption of light in a wide spectral range,

— stability against radiation being absorbed,

— high efficiency of reradiation and weak heating under the action of incident light.

The drawback of QDs is very low mobility of charge carriers, which has a negative impact on the efficiency of solar energy conversion to electricity. To increase the charge carrier mobility, graphene or graphene derivatives are used. The advantages of utilizing graphene in solar cells include:

— unique electrically and heat-conducting properties under normal conditions,

— high charge carrier mobility under normal conditions, and

— low light absorbance in the visible region.

Thus, 2D graphene–QD hybrid structures should exhibit the optical properties of QDs and the transport properties of graphene. In this case, QDs will efficiently absorb solar radiation and generate charge carriers, while graphene will act as conductor of separated photogenerated charge carriers. The graphene–QD solar cells include two electrodes, the EIL and HIL sandwiched between them and one or more layers containing QDs and graphene (Fig. 7).

Recent studies showed that improvement of the properties and efficiency of solar cells based on 2D graphene–QD hybrid structures requires both the search for the most efficient design of particular components of the photoactive layer and injection layers and taking account of the synergistic effect of all other components of the system. In the text below we will analyze all components of solar cells using particular examples, specify general principles of the choice of certain components and formulate problems to be solved in the future.

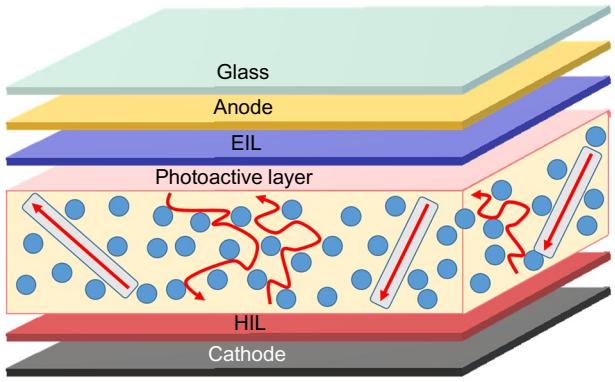


Figure 7. Graphene–QD solar cell: a possible structure. Charge carrier trajectories in the photoactive layer in the presence (straight arrows) and in the absence (bent arrows) of graphene.

The design of solar cells based on graphene–QD hybrids involves the following steps:

— the choice of components for light absorption and charge carrier generation,

— the choice of an improved method for extraction of charge carriers from the photoactive layer, and

— the choice of the substrate and electrode materials and the fashion of electrode attachment.

4.1. The choice of components for light absorption and charge carrier generation

Over a long period of time low charge carrier mobility in QDs precluded fabrication of efficient QD-based solar cells. The charge carrier mobility in QD layers depends on the QD size and composition, on the presence of a shell, on the dopant material , *etc*. For PbS QDs treated with ethane-1,2-dithiol (EDT) this parameter can vary from a few thousandth to a few tenth of $cm^2\ V^{-1}\ s^{-1}$,[101] being almost 100 times lower than in other light-absorbing materials (*cf.* $> 10\ cm^2\ V^{-1}\ s^{-1}$ for CdTe films).[102] The best way to increase the charge carrier mobility in QD layers is to use graphene since it has a record high value of this property, *viz.*, about $2 \times 10^4\ cm^2\ V^{-1}\ s^{-1}$.[103] Owing to its small thickness (monatomic layer) graphene is characterized by very low light absorbance (~2.3%), therefore, incident light is absorbed by the QD layer almost without loss.[104] A proper choice of the method for modification of graphene or graphene derivative, the QD material, structure, composition and shape, as well as the design of graphene–QD hybrid structures are the keys to successful optimization of solar energy absorption and charge transfer processes.

The choice between graphene, GO, reduced graphene oxide (RGO), as well as fluorinated or chlorinated GO and other derivatives is intimately related to the choice of the QD type. Efficient charge transfer from QDs to graphene requires that the energy of the lowest unoccupied molecular orbital (LUMO) of QDs be higher than the lowest energy level of graphene or graphene derivative, as shown in Fig. 8.

Markad *et al.*[105] compared the photoluminescence spectra of QD colloidal solutions, a graphene–QD composite and QD synthesized on graphene surface and found that

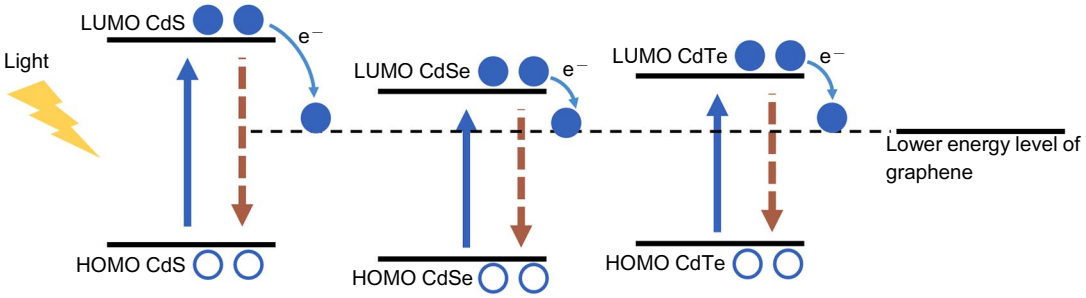


Figure 8. Electron transfer from QDs to graphene: a schematic.
Solid straight arrows denote a HOMO–LUMO transition; dashed straight arrows denote electron return accompanied by fluorescence of QDs; and bent arrows denote electron transfer from QDs to graphene.

efficient energy transfer between QDs and graphene is possible only if QDs are arranged at rather short distance from graphene surface. It was shown that the QD photoluminescence intensity at the graphene surface decreases considerably and that photoluminescence spectrum changes, the effects observed being least pronounced for a physical mixture of graphene and QDs.[105] The absorption spectrum of QDs on graphene surface also changes due to the changes in the energies of the highest occupied molecular orbital (HOMO) and the LUMO and to different HOMO and LUMO energies for QDs.

There is a wide variety of QD types. Indeed, they can differ in size (from a few to several tens of nanometres) and core composition (PbS, CdTe, $CuInS_2$, $AgInS_2$, *etc.*) or have a core/shell structure (*e.g.*, $CuInS_2$/ZnS and $AgInS_2$/ZnS). The surface of quantum dots can be modified with various molecules to make QDs soluble in certain solvents as well as to change their optical and semiconductor properties or the type of immobilization on graphene surface. The QD shape affects their organization on the graphene surface. Light-induced long-lived exciton states of QDs suppress thermal dissipation of absorbed energy and enable efficient utilization of QDs as charge carrier donors for graphene. Shell buildup on QD surface opens a way to minimize dissipation of absorbed energy to heat by elimination of defects on the core surface.

There are two main methods for fabrication of graphene–QD hybrids. One involves incorporation of graphene and QDs into a polymer substrate sandwiched between electrodes to prepare a graphene–QD pseudohybrid. The other is aimed to directly obtain close-packed 2D graphene–QD hybrid structures.

Although the former approach is less efficient (see above), it delivers a positive result, being much more simple and cheap from the standpoint of commercialization as applied to solar cells. For instance, Kim *et al.*[98] reported fabrication of solar cells by the spin coating process. To this end, the pretreated surface of an electrode and an n-type semiconductor is coated with a layer of colloidal PbS QDs coated with oleic acid to prevent the aggregation of nanocrystals and a layer of tetrabutylammonium iodide (TBAI), which is necessary for solid-phase ligand exchange on QD surface and to ensure efficient charge transfer from QDs to graphene. The final stage involves the formation of a p-type semiconductor layer and deposition of a gold electrode. Three solar cells thus fabricated comprised 12 QD layers (sample 1), 12 QD layers and 5 graphene layers (sample 2) and 12 QD layers and 9 graphene layers (sample 3). Although the open-circuit voltage for all cells was almost independent of the presence of the graphene interlayers, the short-circuit current increased substantially and the ECE in turn increased to 6.99%. Photogenerated electrons are transferred to graphene, thus reducing the probability of charge recombination in the QD layers. Optimization of the spin coating technique and the number of graphene layers allowed one to increase the ECE of a solar cell of identical composition to 8.82%.[98]

Yet another solar cell is based on PbS QDs treated with TBAI and EDT.[106] Graphene and chlorinated graphene oxide (Cl-GO) were introduced into the PbS–TBAI and PbS–EDT films, respectively, to impart the properties of a weak n-type semiconductor and a p-type semiconductor to the corresponding hybrid solids. The Cl-GO–PbS film acted as the HIL. This approach enabled transfer of holes only to graphene and Cl-GO, while electrons were reliably blocked. The efficiency of this solar cell was 10.7%.[106]

The method of formation of 2D graphene–QD hybrid materials assumes an initial organization and immobilization of QD on the surface of graphene or graphene derivatives followed by introduction of the hybrid into the polymer substrate and incorporation of the latter into the solar cell structure. For instance, Martín-García *et al.*[107] used covalent linking between QDs and RGO. The surface of RGO was functionalized with 3-mercaptopropyltrimethoxysilane that can bind to both RGO *via* SiO groups and to QDs *via* SH ones. An X-ray photoelectron spectroscopy of the structure of the hybrid material thus fabricated revealed good coverage of the RGO surface with PbS QDs. By varying the RGO/QD ratio it was possible to vary the QD surface density. The possibility to engineer RGO–core/shell QDs (CdSe/CdS) with shells of different shape and thickness was also demonstrated. This was used to study the efficiency of charge transfer from QDs to graphene as function of the separation between them. The efficiency of charge transfer was 94% at a QD shell thickness of about 0.2 nm (*cf.* merely 30% at a thickness of 1.1 nm). As a consequence, the photoluminescence lifetime decreased from 1.4 μs to 66 ns and the photoluminescence intensity decreased by 92%.[107]

Markad *et al.*[105] fabricated an RGO–CdTe QD composite by direct synthesis of QDs on the RGO surface. An X-ray photoelectron spectroscopy revealed a high degree of the RGO surface coverage with QDs and high charge

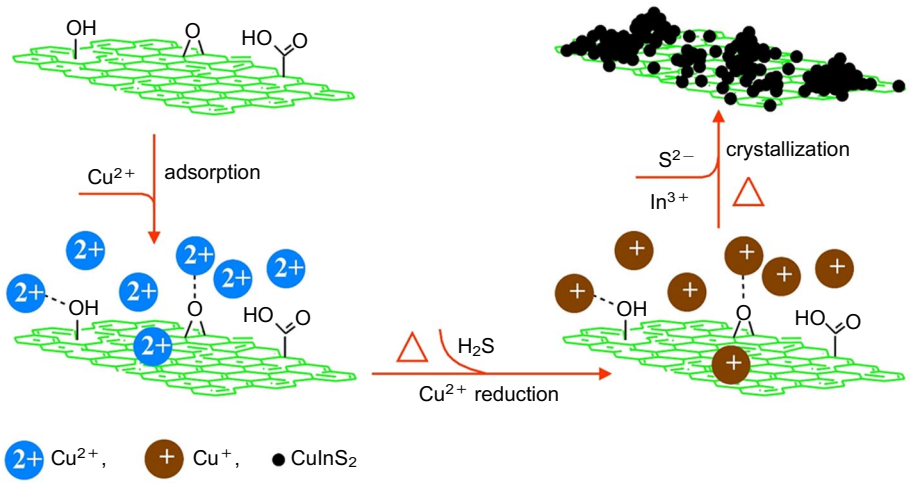


Figure 9. Formation of reduced graphene oxide/QD ($CuInS_2$) hybrid structure.[108] △ denotes heat supply.

Table 2. Research directions and methods for optimization of 2D graphene – QD hybrid structures.

Possible solution	Comments	Ref.
Target: choosing a method for fabrication of graphene – quantum dot hybrid structures		
Fabrication of graphene – QD – polymer composites	The method is simple and cheap; inefficient charge carrier transfer between QDs and graphene; the energy conversion efficiency depends on the polymer chosen and on auxiliary reagents used to fabricate graphene – QD – polymer composites	109 – 111
Fabrication of close-packed 2D graphene – QD hybrid structures followed by incorporation into polymer matrices	Efficient charge carrier transfer between QDs and graphene; the possibility of controlling the process of QD packing on graphene; the energy conversion efficiency depends on the polymer, linker and method used for QD fabrication (colloidal synthesis or assembly of QDs on graphene surface)	98, 107, 112
Combination	Fabrication of graphene – QD hybrid structures using (i) various types of QDs and graphene modifications and (ii) various methods for the formation of nanocomposites within the photoactive layer	113
Target: choosing a pair of quantum dots and a graphene derivative		
Proper choice of a pair of quantum dots and a graphene derivative	One should choose between various types of QDs and graphene derivatives based on energy level diagram taking account of the nature of ligands and linkers, the method for fabrication of hybrid structures and principles of charge carrier transfer; the most promising pairs of semiconductor QDs include PbS (PbSe) and $CuInS_2$ ($AgInS_2$) on the surface of graphene or RGO	75, 114 – 117
Target: fabrication of quantum dots		
Colloidal synthesis of QDs	One should choose the core and shell materials, the shape of the shell, and chemical compounds for functionalization of graphene surface and ligands. The advantage of the method consists in that colloidal QDs can be incorporated with ease into various polymer matrices and coated on graphene surface	118, 119
Synthesis of QDs on graphene surface	Key drawback: weak control of QD parameters, which complicates the interpretation of results obtained	108
Target: choosing a graphene derivative		
Preliminary modification of graphene followed by formation of a hybrid with QDs	One should choose (i) between graphene, graphene oxide, RGO and functionalized derivatives and (ii) a proper method of fabrication. The approach is more flexible and technologically simple	85, 120, 121

transfer efficiency evaluated from changes in the QD fluorescence intensity and the QD fluorescence decay time.

Meng *et al.*[108] described an approach involving simultaneous reduction of GO and synthesis of $CuInS_2$ QDs on GO surface (Fig. 9). Using the hybrid material thus prepared and poly[1-methoxy-4-(2-ethylhexyloxy)-*p*-phenylenevinylene], a solar cell with improved open-circuit voltage (V_{oc}) and short-circuit current was fabricated.

Examples mentioned above and the principles of the choice of optimum methods for fabrication of graphene – QD hybrid structures, the type of QDs and particular graphene form, as well as the most appropriate linkers and polymers are collected in Table 2.

4.2. Methods for improvement of charge carrier extraction from the photoactive layer

The efficiency of hybrid solar cells is not very high due to low V_{oc}. Theoretically, the maximum V_{oc} value equals the energy difference between the electron acceptor (graphene) LUMO and the electron donor (QD) HOMO; however, real voltages V_{oc} are lower because of the dark current, charge carrier recombination and incomplete splitting of the acceptor and donor Fermi levels. To reduce the influence of negative factors and, therefore, to increase V_{oc}, layered structures containing the HIL and EIL are prepared (Fig. 10).

This is necessary to minimize the energy barriers for charge extraction (including selective extraction) and, unlike other structures where V_{oc} is limited by not only the properties of the donors and acceptors, but also the energy levels of the electrode materials, allows one to increase V_{oc}. With a proper choice of the layer materials for electron and hole collection, the voltage V_{oc} is determined by the properties of QDs and graphene.

Utilization of the layers in question primarily concerns:

— the minimization of the energy barriers in order to extract charge carriers, which leads to an increase in V_{oc};

— the selective extraction of a charge carrier type and blocking of the opposite one, thus reducing the excitation decay;

— the increase in the efficiency of absorption of solar energy;

— the improvement of the contacts between the electrodes and the photoactive layer and the smoothness of the interfaces between them in order to stabilize processes occurring in the photoactive layer.

The role of the EIL is played by ZnO, LiF or GO derivatives, while poly(3,4-ethylenedioxythiophene) polystyrene sulfonate (PEDOT:PSS), or GO act as the HIL.

When preparing the EIL and HIL, Liu *et al.*[122] used GO derivatives and caesium for electron transport to the cathode; Yang *et al.*[123] used Cs_2CO_3-functionalized graphene QDs, while Jayawardena *et al.*[124] utilized RGO functionalized with ZnO or TiO_2. Emphasize that the introduction of graphene into these compounds, which are traditionally used to prepare the EIL, allowed one to increase the ECE from 7.39% to 7.50% using ZnO (additional functionalization of the modified surface with ethylcellulose increased the ECE to 8.4%) and from 7.22% to 7.46% using TiO_2.[125] Graphene can also be modified with fullerenes and lithium.[126] The modification is necessary to match the HIL and the HOMO of the hole donor polymer and to improve the hole transport properties.

A 2-nm thick GO layer is a good alternative to PEDOT:PSS.[127] Subsequent increase in the number of graphene layers to a thickness of 10 nm causes a significant decrease in the fill factor and in the overall efficiency of solar cells. Besides, the use of RGO[128] or partially reduced GO with the polymer PTB7§ as donor causes an increase in the cell efficiency.[129] Yuan *et al.*[130] prepared a composite

§ Poly({4,8-bis[(2-ethylhexyl)oxy]benzo[1,2-*b*:4,5-*b*′]dithiophene-2,6-diyl}{3-fluoro-2-[(ethylhexyl)carbonyl]thieno[3,4-*b*]thiophenediyl}).

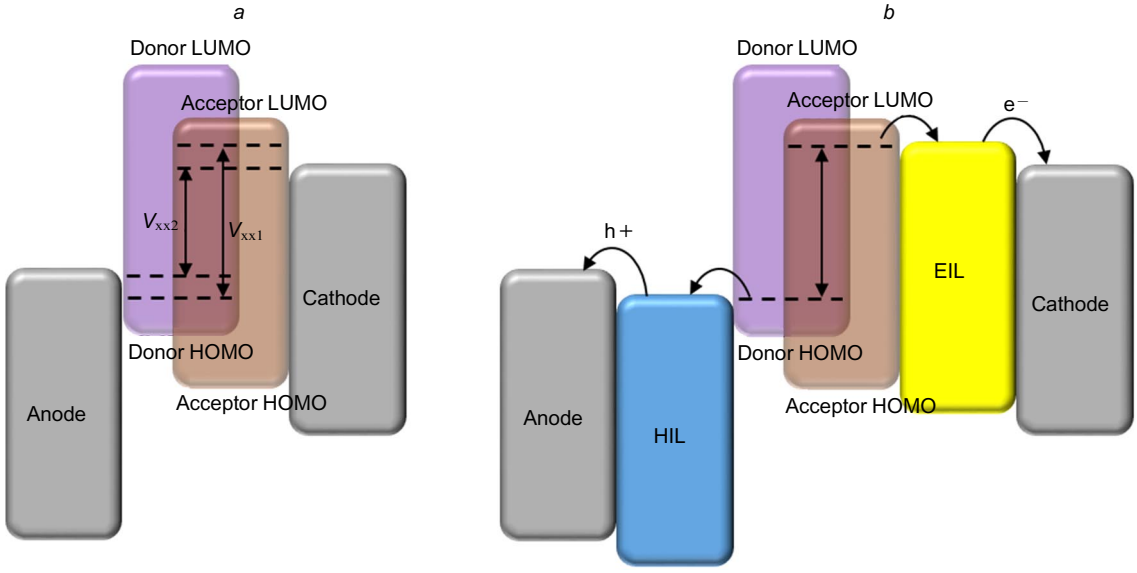


Figure 10. Energy level diagram and transport of charge carriers within a solar cell (adapted from Ref. 12). Without charge extraction layers (*a*) and with charge extraction layers (*b*).

from PEDOT:PSS and layers containing GO and silver nanoparticles and demonstrated a 15% increase in the cell efficiency. Complexes of GO with gold nanoparticles give a 16% increase in the efficiency compared to that of solar cells fabricated using no gold nanoparticles.[131] Very good results were obtained using the HIL prepared from GO that was reduced with sulfates and then surface-decorated with, *e.g.*, OSO_3H groups. The ECE of solar cells with this HIL is as high as 4.37%, being only 0.02% lower compared with the solar cells with the PEDOT:PSS layer.[132] No abrupt increase in the efficiency of solar cells with the HIL based on graphene derivatives compared to that of cells with the PEDOT:PSS-based HIL has been reported so far; however, it was shown that the HILs based on GO derivatives are much more stable.

Two more methods for increasing the efficiency of the GO-based HIL involve tuning the energy level by functionalization of the GO surface with fluorine[133] and preparation GO with specified degree of oxidation using controlled sequence of pre-oxidation steps, choice of reagents and duration of the oxidation process. The technique allows one to vary the work function of GO between 4.74 and 5.06 eV.[134] Both methods proved themselves. An alternative controlled oxidation approach is based on γ-irradiation of GO in aqueous ethanol.[135]

Stratakis *et al.*[136] used laser-induced doping of GO in the presence of precursor gas. Taking doping of GO with chlorine as an example, it was shown that chlorine atoms form covalent C – Cl bonds at both sides of the graphene sheet, thus ensuring an increase in the work function from 4.91 to 5.23 eV.

Thus, methods for improvement of charge carrier extraction from the photoactive layer are closely related not only to the composition and properties of the HIL and EIL, but also to graphene modification. The key avenues of research activity in this field and possible solutions are summarized in Table 3.

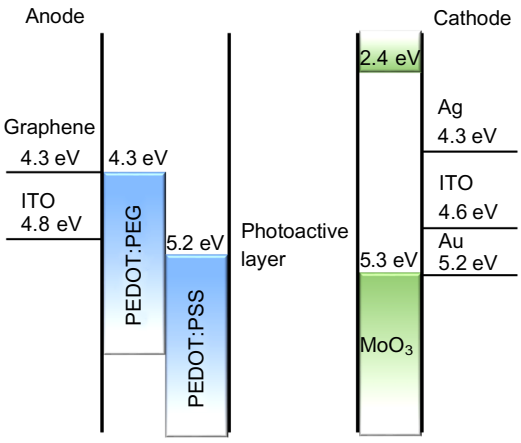


Figure 11. Energy level diagrams for various types of anodes and cathodes.[148]

4.3. The choice of the substrate and electrode materials and the fashion of electrode attachment

Considerable attention is paid to the type and arrangement of electrodes for voltage dump. Usually, one electrode (namely, photoanode) should be transparent to incident light to transmit the luminous flux without loss; the photocathode can be opaque. Electrons are transferred from the material with lower work function to the material with higher work function; therefore, it is clear that the work function of the electrode material will also influence the efficiency of solar cells. The work functions of various types of electrodes are compared in a diagram shown in Fig. 11.[148] Table 4 lists the work functions of electrode materials for solar cells.

In most cases the photoanode is fabricated from ITO coated on transparent glass, SiO_2 or TiO_2 substrates. Indium – tin oxide exhibits the properties of a semiconduc-

Table 3. Methods to improve extraction of charge carriers from the photoactive layer.

Possible solution	Comments	Ref.
	Target: choosing the method for electron extraction	
A system without EIL	Thorough choice of electrodes and electrode surface polishing is required; low V_{oc} causes a significant decrease in the solar cell efficiency	137, 138
A system with EIL based on chemical compounds	The approach proved itself in various types of solar cells; high performance and simplicity of EIL fabrication. This type of EIL is less stable than graphene-based EIL. Possible structures are chosen taking account of the cathode material	139, 140
Systems with EIL based on graphene derivatives	These EIL are more stable than the EIL based on traditionally used chemical compounds, exhibit high performance; RGO and its derivatives as well as graphene QDs are used	141 – 143
	Target: choosing a hole extraction technique	
A system without HIL	Thorough choice of electrodes and surface polishing is required; low V_{oc} leads to significant decrease in the solar cell efficiency	138
A system with HIL based on chemical compounds	High efficiency and great experience in application of these HILs, low cost; lower stability compared to HIL based on graphene derivatives. Traditionally used system PEDOT:PSS	144, 145
Systems with EIL based on graphene derivatives	Complicated HIL fabrication methods; HIL efficiency is identical to that of the HIL based on chemical compounds; high stability. Usually, graphene oxide and its derivatives are utilized	132, 146, 147

Table 4. Work function values for electrode materials used in solar cells.

Electrode material	Work function /eV	Ref.	Electrode material	Work function /eV	Ref.
Au	5.2	148	$SrTiO_3$	4.26	153
Ag	4.3	148	Ni	5.04	154
Nb_2O_5	3.4	149	TiO_2	4.3	155
Zn_2SnO_4	3.6	149	Pt	5.65	156
Single-layered graphene	4.8	150	ZnO:Al	4.62	157
Multilayered graphene	5.0	150	ZnO	4.71	157
SnO_2	4.1 – 5.7	151	CuO	7.8	158
PEDOT:PSS	5.0 – 5.2	152			

Table 5. Methods for choosing photoanode and photocathode materials.

Possible solution	Comments	Ref.
	Target: choosing a photoanode	
The use of conventional materials	Traditionally used materials provide good transparency and high energy conversion efficiency of solar cells and are characterized by high incident radiation reflectance in the IR range	167, 168
The use of materials based on graphene derivatives	Materials based on graphene derivatives provide an identical performance compared to the traditionally used materials; they allow IR radiation to pass to the photoactive layers. A preferred strategy is to use RGO and its complexes with various compounds	169, 170
	Target: choosing a photocathode	
The use of conventional materials	Traditionally used materials provide high energy conversion efficiency of solar cells and are widely used in manufacturing; however, they are characterized by low optical transparency or are opaque	171, 172
Application of materials based on graphene derivatives	Materials based on graphene derivatives are optically transparent and can be used for fabrication of transparent solar cells; graphene on glass and quartz substrates can be utilized in hybrid solar cells	169, 173

tor and has a wide band gap ($\sim$4 eV). The drawback of the ITO photoanodes includes high IR reflectivity, which considerably decreases the luminous flux and the efficiency of the light harvesting process. Other materials include aluminium – zinc oxide and tin oxide doped with fluorine or antimony. Recently, graphene has been used as photoanode; the efficiency of the ITO-based solar cells is higher.[159] In solar cells, the ITO layer is usually in contact with the PEDOT:PSS film that is spin coated onto plasma-pretreated ITO surface. The choice of a certain type of the photoanode is closely related to the type of the HIL used, namely, a decrease in the homogeneity of the PEDOT:PSS film coated onto graphene can cause a considerable increase in resistance. Efficient contact between the graphene anode and the HIL based on PEDOT:PSS can be achieved by doping graphene with AuCl; for MoO_3-based anodes this can be done by doping the anode with hydrochloric and nitric acids.[160] Besides, contacts can be improved using surfactant additives to change the hydrophobicity of the materials.[161] Thus, the choice of the photoanode material is closely related to the type and composition of solar cells.

If there is no need for a transparent photocathode, metals including aluminium, silver, gold, *etc*., are used. Otherwise, transparent photocathodes for multilayer or transparent solar cells can be fabricated from tin oxide doped with fluorine and graphene nanoparticles, the transparency of such electrodes can exceed 85%.[162] However, graphene-based electrodes are still of limited use even in the laboratory practice owing to low efficiency of solar cells based on them. Photocathodes are also fabricated from platinum-doped polymers; but they are expensive and the search for novel efficient optically transparent materials is relevant. Platinum can be replaced by carbon compounds. For instance, one of the best carbon-based photocathodes provides an ECE of 7.59%.[163] Although modern graphene-based photocathodes with an efficiency of less than 5% (see Ref. 164) require thorough choice of electrolytes, they are considered as the most promising materials for fabrication of transparent solar cells.

Undoubtful advantages of the use of graphene and its derivatives include well-developed layer-transfer methods. This allows one to fabricate electrodes on flexible substrates for transparent, flexible solar cells that are stable against the action of physical factors.[165] Such cells can have a large surface area.[166] Main research trends and approaches to optimization of the choice of the photoanode and photocathode materials are listed in Table 5.

5. Conclusion

When analyzing the examples presented above, mention should be made that unique properties of modern nanomaterials, *viz*. graphene and QDs, can help to significantly improve the efficiency and stability of solar systems. Graphene can be used as a component of almost all functional units in solar cells, that is, (i) an efficient carrier of photo-

generated charges in the photoactive layer; (ii) a HIL and EIL whose stability and efficiency are comparable with those of traditionally used compounds; and (iii) an electrode material due to high transparency and flexibility. The stability of graphene against environmental factors and solar light, first, significantly extends the operating cycle of solar cells and, second, opens the way to large-area transparent solar cells. Low cost of graphene production and simplicity of methods for graphene incorporation into the structure of solar cells allow one to reduce the overall cost of solar systems and make them more commercially competitive. Further research should involve the following:

— simulation of the energy spectra of 2D graphene – QD hybrid structures and processes of nonradiative charge transfer from QDs to graphene;

— an analysis of the influence of QD ligands on the morphological, optical and electronic properties of 2D structures in order to determine optimum combinations and methods for fabrication of graphene – QD hybrid structures;

— development of novel approaches and methods for graphene modification to optimize the structure of the energy levels, to improve the properties of ohmic contacts, to reduce the cost of high-precision modification of graphene and to increase the number of methods for the introduction of this material into solar cells;

— development of advanced types of QDs (including heavy-metal-free QDs) in order to design environmentally clean manufacturing of solar cells; and

— thorough choice of surface ligands and optimal shell for QDs to reduce charge carrier recombination and to improve charge transfer to graphene.

Progress in these research directions will help to solve key problems in solar power engineering, namely:

— an increase in solar cell efficiency,

— improvement of the reliability and stability of solar cells against environmental factors,

— extension of operating life,

— reductions in toxicity of manufacturing,

— simplification of reclamation or recycling, and

— simplification of fabrication technology and cost reduction of solar cell components.

In this review we demonstrated how these and many other issues are solved using graphene – QD hybrid structures for solar cell applications, analyzed the main trends in the improvement of their properties and formulated topical problems to be solved in the future.

The review has been written with the financial support from the Federal Target Programme of the Ministry of Science and Higher Education of the Russian Federation (Contract No. 14.584.21.0032, Project ID RFMEF158417X0032).

Figure 1 is courtesy of the US National Renewable Energy Laboratory (NREL). Figures 5 and 9 are courtesy of Elsevier. Figure 6 is courtesy of The American Chemical Society. Figure 11 is courtesy of Nature.

References

1. O.Morton. *Nature (London)*, **443**, 19 (2006)
2. B.Dudley. *BP Statistical Review of World Energy*. (66 Edn), 1 (2017)
3. M.A.Green, Y.Hishikawa, E.D.Dunlop, H.D.Levi, J.Hohi-Ebinger, A.W.Y.Ho-Baillie. *Prog. Photovolt.*, **26**, 427 (2018)
4. K.S.Novoselov, A.K.Geim, S.V.Morozov, D.Jiang, Y.Zhang, S.V.Dubonos, I.V.Grigorieva, A.A.Firsov. *Science*, **306**, 666 (2004)
5. Q.Zhang, E.Uchaker, S.L.Candelaria, G.Cao. *Chem. Soc. Rev.*, **42**, 3127 (2013)
6. O.E.Semonin, J.M.Luther, S.Choi, H.Y.Chen, J.Gao, A.J.Nozik, M.C.Beard. *Science*, **334**, 1530 (2011)
7. S.Sharma, K.K.Jain, A.Sharma. *Mater. Sci. Appl.*, **6**, 1145 (2015)
8. J.Jean, P.R.Brown, R.L.Jaffe, T.Buonassisi, V.Bulović. *Energy Environ. Sci.*, **8**, 1200 (2015)
9. H.Akiyama, L.Zhu, M.Yoshita, C.Kim, S.Chen, T.Mochizuki, Y.Kanemitsu. In *Physics, Simulation, and Photonic Engineering of Photovoltaic Devices IV. (Ser. Proceedings of SPIE*. Vol. 9358). (Bellingham, WA: SPIE — the International Society for Optical Engineering, 2015). No. 93580B
10. https://www.nrel.gov/pv/assets/images/efficiency-chart.png (28.10.2018)
11. S.Paulo, E.Palomares, E.Martinez-Ferrero. *Nanomaterials*, **6** (9), 157 (2016)
12. N.Balis, E.Stratakis, E.Kymakis. *Mater. Today*, **19**, 580 (2016)
13. T.Sogabe, Q.Shen, K.Yamaguchi. *J. Photon. Energy*, **6**, 040901 (2016)
14. G.H.Carey, A.L.Abdelhady, Z.Ning, S.M.Thon, O.M.Bakr, E.H.Sargent. *Chem. Rev.*, **115**, 12732 (2015)
15. O.E.Semonin, J.M.Luther, M.C.Beard. *Mater. Today*, **15**, 508 (2012)
16. T.Işik. Thesis for Bachelor. Isik University, Istanbul, 2015. 10.13140/RG.2.1.4298.6404 https://www.researchgate.net/publication/276423464_Solar_Cells_review
17. M.Aghaei. In *Proceedings National Graduate Conference (Natbrad 2012). Universiti Tenaga Nasional, Selangor, Malaysia,* 2012
18. W.A.Badawy. *J. Adv. Res.*, **6**, 123 (2015)
19. S.Kim, J.-W.Chung, H.J.Lee, J.Park, Y.Heo, H.-M.Lee. *Sol. Energy Mater. Sol. Cells*, **119**, 26 (2013)
20. T.D.Lee, A.U.Ebong. *Renew. Sust. Energ. Rev.*, **70**, 1286 (2017)
21. M.Taguchi, A.Terakawa, E.Maruyama, M.Tanaka. *Prog. Photovolt.: Res. Appl.*, **13**, 481 (2005)
22. F.Meneguzzo, R.Ciriminna, L.Albanese, M.Pagliaro. *Energy Sci. Eng.*, **3**, 499 (2015)
23. P.Jackson, D.Hariskos, R.Wuerz, O.Kiowski, A.Bauer, T.M.Friedlmeier, M.Powalla. *Phys. Status Solidi (RRL)*, **9**, 28 (2015)
24. A.Morales-Acevedo. *Solar Energy*, **80**, 675 (2006)
25. S.Philipps. *Photovoltaics Report. PSE Conferences and Consulting GmbH. Fraunhofer ISE, 2018*; https://www.ise.fraunhofer.de/content/dam/ise/de/documents/publications/studies/Photovoltaics-Report.pdf
26. B.O'Regan, M.Grätzel. *Nature (London)*, **353**, 737 (1991)
27. H.J.Snaith, L.Schmidt-Mende. *Adv. Mater.*, **19**, 3187 (2007)
28. A.Hagfeldt, G.Boschloo, L.Sun, L.Kloo, H.Pettersson. *Chem. Rev.*, **110**, 6595 (2010)
29. Y.He, Y.Li. *Phys. Chem. Chem. Phys.*, **13**, 1970 (2011)
30. A.Wadsworth, M.Moser, A.Marks, M.S.Little, N.Gasparini, C.J.Brabec, D.Baran, I.McCulloch. *Chem. Soc. Rev.* (2018); DOI: 10.1039/c7cs00892a
31. D.Perganti, A.G.Kontos, T.Stergiopoulos, V.Likodimos, J.Farnell, D.Milliken, H.Desilvestro, P.Falaras. *Electrochim. Acta*, **179**, 241 (2015)
32. S.Erten-Ela, S.Gokhan Colak, K.Ocakoglu. *Inorg. Chim. Acta*, **405**, 252 (2013)
33. A.Kojima, K.Teshima, Y.Shirai, T.Miyasaka. *J. Am. Chem. Soc.*, **131**, 6050 (2009)
34. W.Nie, H.Tsai, R.Asadpour, J.-C.Blancon, A.J.Neukirch, G.Gupta, J.J.Crochet, M.Chhowalla, S.Tretiak, M.A.Alam, H.-L.Wang, A.D.Mohite. *Science*, **347**, 522 (2015)

35. D.Liu, M.K.Gangishetty, T.L.Kelly. *J. Mater. Chem., A*, **2**, 19873 (2014)
36. G.Tong, H.Li, G.Li, T.Zhang, C.Li, L.Yu, J.Xu, Y.Jiang, Y.Shi, K.Chen. *Nano Energy*, **48**, 536 (2018)
37. L.K.Ono, E.J.Juarez-Perez, Y.Qi. *ACS Appl. Mater. Interfaces*, **9**, 30197 (2017)
38. J.M.Ball, M.M.Lee, A.Hey, H.J.Snaith. *Energy Environ. Sci.*, **6**, 1739 (2013)
39. Y.Rong, Y.Hu, A.Mei, H.Tan, M.I.Saidaminov, S.I.Seok, M.D.McGehee, E.H.Sargent, H.Han. *Science*, **361**, 1214 (2018)
40. Z.Shi, A.H.Jayatissa. *Materials*, **11**, 729 (2018)
41. M.I.Asghar, J.Zhang, H.Wang, P.D.Lund. *Renew. Sust. Energy Rev.*, **77**, 131 (2017)
42. F.T.F.O'Mahony, Y.H.Lee, C.Jellett, S.Dmitrov, D.T.J.Bryant, J.R.Durrant, B.C.O'Regan, M.Graetzel, M.K.Nazeeruddin, S.A.Haque. *J. Mater. Chem., A*, **3**, 7219 (2015)
43. E.Stratakis, E.Kymakis. *Mater. Today*, **16**, 133 (2013)
44. C.-C.Chen, W.-H.Chang, K.Yoshimura, K.Ohya, J.You, J.Gao, Z.Hong, Y.Yang. *Adv. Mater.*, **26**, 5670 (2014)
45. A.P.Litvin, I.V.Martynenko, F.Purcell-Milton, A.V.Baranov, A.V.Fedorov, Y.K.Gun'ko. *J. Mater. Chem. A*, **5**, 13252 (2017)
46. J.J.Choi, W.N.Wenger, R.S.Hoffman, Y.-F.Lim, J.Luria, J.Jasieniak, J.A.Marohn, T.Hanrath. *Adv. Mater.*, **23**, 3144 (2011)
47. A.J.Labelle, S.M.Thon, S.Masala, M.M.Adachi, H.Dong, M.Farahani, A.H.Ip, A.Fratalocchi, E.H.Sargent. *Nano Lett.*, **15**, 1101 (2015)
48. Z.Yang, J.Z.Fan, A.H.Proppe, F.P.G.de Arquer, D.Rossouw, O.Voznyy, X.Lan, M.Liu, G.Walters, R.Quintero-Bermudez, B.Sun, S.Hoogland, G.A.Botton, S.O.Kelley, E.H.Sargent. *Nat. Commun.*, **8**, 1325 (2017)
49. E.M.Sanehira, A.R.Marshall, J.A.Christians, S.P.Harvey, P.N.Ciesielski, L.M.Wheeler, P.Schulz, L.Y.Lin, M.C.Beard, J.M.Luther. *Sci. Adv.*, **3**, eaao04204 (2017)
50. C.S.S.Sandeep, S.ten Cate, J.M.Schins, T.J.Savenije, Y.Liu, M.Law, S.Kinge, A.J.Houtepen, L.D.A.Siebbeles. *Nat. Commun.*, **4**, 2360 (2013)
51. S.Li, L.Ye, W.Zhao, H.Yan, B.Yang, D.Liu, W.Li, H.Ade, J.Hou. *J. Am. Chem. Soc.*, **140**, 7159 (2018)
52. G.Armstrong. *Nat. Chem.*, **4**, 4 (2011)
53. P.Li, C.Chen, J.Zhang, S.Li, B.Sun, Q.Bao. *Front. Mater.*, **1**, Article 26 (2014)
54. R.Garg, S.Elmas, T.Nann, M.R.Andersson. *Adv. Eng. Mater.*, **7**, 1601393 (2017)
55. A.Rakovich, A.Sukhanova, N.Bouchonville, E.Lukashev, V.Oleinikov, M.Artemyev, V.Lesnyak, N.Gaponik, M.Molinari, M.Troyon, Y.P.Rakovich, J.F.Donegan, I.Nabiev. *Nano Lett.*, **10**, 2640 (2010)
56. E.P.Kolesova, A.O.Orlova, V.G.Maslov, Yu.K.Gun'ko, O.Cleary, A V Baranov, A.V.Fedorov, *Opt. Spectrosc.*, **125** (1), 99 (2018)
57. V.Renugopalakrishnan, B.Barbiellini, C.King, M.Molinari, K.Mochalov, A.Sukhanova, I.Nabiev, P.Fojan, H.L.Tuller, M.Chin, P.Somasundaran, E.Padrós, S.Ramakrishna. *J. Phys. Chem. C*, **118**, 16710 (2014)
58. S.Dayneko, A.Tameev, M.Tedoradze, I.Martynov, M.Artemyev, I.Nabiev, A.Chistyakov. *Appl. Phys. Lett.*, **103**, 063302 (2013)
59. G.D.Scholes. *J. Am. Chem. Soc.*, **130**, 18028 (2008)
60. C.deMello Donegá. *Chem. Soc. Rev.*, **40**, 1512 (2011)
61. M.N.Kalasad, M.K.Rabinal, B.G.Mulimani. *Langmuir*, **25**, 12729 (2009)
62. H.Han, G.Di Francesco, M. M.Maye. *J. Phys. Chem. C*, **114**, 19270 (2010)
63. M.Protiere, N.Nerambourg, O.Renard, P.Reiss. *Nanoscale Res. Lett.*, **6**, 472 (2011)
64. J.J.Li, Y.A.Wang, W.Guo, J.C.Keay, T.D.Mishima, M.B.Johnson, X.Peng. *J. Am. Chem. Soc.*, **125**, 12567 (2003)
65. P.A.Linkov, K.V.Vokhmintcev, P.S.Samokhvalov, M.Laronze-Cochard, J.Sapi, I.R.Nabiev. In *The 2nd International Symposium Physics, Engineering and Technologies for Biomedicine. (Book of Abstracts). Mocow, 2018*. P. 194
66. P.S.Samokhvalov, P.A.Linkov, M.A.Zvaigzne, A.V.Kosmynceva, I.O.Petrova, V.A.Krivenkov, A.V.Sukhanova, I.R. Nabiev. In *The 2nd International Symposium Physics, Engineering and Technologies for Biomedicine (Book of Abstracts). Mocow, 2018*. P. 449
67. P.Reiss, M.Protiere, L.Li. *Small*, **5**, 154 (2009)
68. K.V.Vokhmintcev, P.S.Samokhvalov, I.Nabiev. *Nano Today*, **11**, 189 (2016)
69. P.Samokhvalov, M.Artemyev, I.Nabiev. *Chem. – Eur. J.*, **19**, 1534 (2013)
70. M.A.Zvaigzne, I.L.Martynov, P.S.Samokhvalov, I.R.Nabiev. *Russ. Chem. Bull, Int. Ed.*, **65**, 2568 (2016)
71. M.Samadpour. *Solar Energy*, **144**, 63 (2017)
72. D.So, S.Pradhan, G.Konstantatos. *Nanoscale*, **8**, 16776 (2016)
73. M.G.Panthani, C.J.Stolle, D.K.Reid, D.J.Rhee, T.B.Harvey, V.A.Akhavan, Y.Yu, B.A.Korgel. *J. Phys. Chem. Lett.*, **4**, 2030 (2013)
74. S.M.Kobosko, D.H.Jara, P.V.Kamat. *ACS Appl. Mater. Interfaces*, **9**, 33379 (2017)
75. J.Du, Z.Du, J.-S.Hu, Z.Pan, Q.Shen, J.Sun, D.Long, H.Dong, L.Sun, X.Zhong, L.-J.Wan. *J. Am. Chem. Soc.*, **138**, 4201 (2016)
76. K.Tvrdy, P.A.Frantsuzov, P.V.Kamat. *Proc. Natl. Acad. Sci.*, **108**, 29 (2011)
77. M.Eizenberg, J.M.Blakely. *Surf. Sci.*, **82**, 228 (1979)
78. N.Liu, F.Luo, H.Wu, Y.Liu, C.Zhang, J.Chen. *Adv. Funct. Mater.*, **18**, 1518 (2008)
79. N.Behabtu, J.R.Lomeda, M.J.Green, A.L.Higginbotham, A.Sinitskii, D.V.Kosynkin, D.Tsentalovich, A.N.Parra-Vasquez, J.Schmidt, E.Kesselman, Y.Cohen, Y.Talmon, J.M.Tour, M.Pasquali. *Nat. Nanotechnol.*, **5**, 406 (2010)
80. P.W.Sutter, J.-I.Flege, E.A.Sutter. *Nat. Mater.*, **7**, 406 (2008)
81. E.Dervishi, Z.Li, F.Watanabe, A.Biswas, Y.Xu, A.R.Biris, V.Saini, A.S.Biris. *Chem. Commun.*, 4061 (2009)
82. C.-D.Kim, B.-K.Min, W.-S.Jung. *Carbon*, **47**, 1610 (2009)
83. M.S.A.Bhuyan, M.N.Uddin, M.M.Islam, F.A.Bipasha, S.S.Hossain. *Int. Nano Lett.*, **6**, 65 (2016)
84. X.-Y.Wang, A.Narita, K.Müllen. *Nat. Rev. Chem.*, **2**, 0100 (2017)
85. S.P.Lonkar, Y.S.Deshmukh, A.A.Abdala. *Nano Res.*, **8**, 1039 (2015)
86. D.-W.Lee, T.Kim, M.Lee. *Chem. Commun.*, **47**, 8259 (2011)
87. J.Liu, L.Tao, W.Yang, D.Li, C.Boyer, R.Wuhrer, F.Braet, T.P.Davis. *Langmuir*, **26**, 10068 (2010)
88. T.Zhang, Z.Cheng, Y.Wang, Z.Li, C.Wang, Y.Li, Y.Fang. *Nano Lett.*, **10**, 4738 (2010)
89. I.A.Reznik, Y.A.Gromova, A.S.Zlatov, M.A.Baranov, A.O.Orlova, S.A.Moshkalev, V.G.Maslov, A.V.Baranov, A.V.Fedorov. *Opt. Spectrosc.*, **122** (1), 114 (2017)
90. S.Stankovich, D.A.Dikin, G.H.Dommett, K.M.Kohlhaas, E.J.Zimney, E.A.Stach, R.D.Piner, S.T.Nguyen, R.S.Ruoff. *Nature (London)*, **442**, 282 (2006)
91. Y.A.Gromova, A.V.Alaferdov, V.A.Ermakov, K.V.Bogdanov, I.V.Martynenko, A.O.Orlova, V.G.Maslov, S.A.Moshkalev, A.V.Baranov, A.V. Fedorov. In *Nanophotonics V. (Ser. Proceedings of SPIE*. Vol. 9126). (Bellingham, WA: SPIE — the International Society for Optical Engineering, 2014). No. UNSP 91262K
92. I.A.Reznik, Y.A.Gromova, A.S.Zlatov, M.A.Baranov, A.O.Orlova, S.A.Moshkalev, V.G.Maslov, A.V.Baranov, A.V.Fedorov. In *Nanophotonics VI. (Ser. Proceedings of SPIE*. Vol. 9884). (Bellingham, WA: SPIE — the International Society for Optical Engineering, 2014). No. 9884A
93. J.Liu, J.Tang, J.J.Gooding. *J. Mater. Chem.*, **22**, 12435 (2012)

94. F.S.Ghoreishi, V.Ahmadi, M.Samadpour. *J. Power Sources*, **271**, 195 (2014)
95. C. X.Guo, H.B.Yang, Z.M.Sheng, Z.S.Lu, Q. L.Song, C.M.Li. *Angew. Chem., Int. Ed.*, **49**, 3014 (2010)
96. D.Barpuzary, M.Qureshi. *ACS Appl. Mater. Interfaces*, **5**, 11673 (2013)
97. Y.Zhu, X.Meng, H.Cui, S.Jia, J.Dong, J.Zheng, J.Zhao, Z.Wang, L.Li, L.Zhang, Z.Zhu. *ACS Appl. Mater. Interfaces*, **6**, 13833 (2014)
98. B.-S.Kim, D.C.J.Neo, B. Hou, J.B.Park, Y.Cho, N.Zhang, J.Hong, S.Pak, S.Lee, J.I.Sohn, H.E.Assender, A.A.R.Watt, S.Cha, J.M.Kim. *ACS Appl. Mater. Interfaces*, **8**, 13902 (2016)
99. F.Rana. *Phys. Rev. B*, **76**, 155431 (2007)
100. F.Rana, P.A.George, J.H.Strait, J.Dawlaty, S.Shivaraman, M.Chandrashekhar, M.G.Spencer. *Phys. Rev. B*, **79**, 115447 (2009)
101. C.-H.M.Chuang, A.Maurano, R.E.Brandt, G.W.Hwang, J.Jean, T.Buonassisi, V.Bulovič, M.G.Bawendi. *Nano Lett.*, **15**, 3286 (2015)
102. M.Grätzel. *Nat. Mater.*, **13**, 838 (2014)
103. C.-H.Liu, Y.-C.Chang, T.B.Norris, Z.Zhong. *Nat. Nanotechnol.*, **9**, 273 (2014)
104. R.R.Nair, P.Blake, A.N.Grigorenko, K.S.Novoselov, T.J.Booth, T.Stauber, N.M.Peres, A.K.Geim. *Science*, **320**, 1308 (2008)
105. G.B.Markad, S.Battu, S.Kapoor, S.K.Haram. *J. Phys. Chem. C*, **117**, 20944 (2013)
106. L.Hu, D.-B.Li, L.Gao, H.Tan, C.Chen, K.Li, M.Li, J.-B.Han, H.Song, H.Liu, J.Tang. *Adv. Funct. Mater.*, **26**, 1899 (2016)
107. B.Martín-Garcìa, A.Polovitsyn, M.Prato, I.Moreels. *J. Mater. Chem., C*, **3**, 7088 (2015)
108. W.Meng, X.Zhou, Z.Qiu, C.Lium J.Chen, W.Yue, M.Wang, H.Bi. *Carbon*, **96**, 532 (2016)
109. D.Arthisree, G.M.Joshi. *J. Mater. Sci.: Mater. Electron.*, **28**, 10516 (2017)
110. H.B.Yang, Y.Q.Dong, X.Wang, S.Y.Khoo, B.Liu, C.M.Li. *Sol. Energy Mater. Sol. Cells*, **117**, 214 (2013)
111. C.V.Pham, A.F.Madsuha, T.V.Nguyen, M.Krueger. *Synth. Met.*, **219**, 33 (2016)
112. Q.Nian, L.Gao, Y.Hu, B.Deng, J.Tang, G.J.Cheng. *ACS Appl. Mater. Interfaces*, **9**, 44715 (2017)
113. L.Tong, F.Qiu, T.Zeng, J.Long, J.Yang, R.Wang, J.Zhang, C.Wang, T.Sun, Y.Yang. *RSC Adv.*, **7**, 47999 (2017)
114. N.Zhao, T.P.Osedach, L.-Y.Chang, S.M.Geyer, D.Wanger, M.T.Binda, A.C.Arango, M.G.Bawendi, V.Bulovič. *ACS Nano*, **4**, 3743 (2010)
115. D.-K.Ko, A.Maurano, S.K.Suh, D.Kim, G.W.Hwang, J.C.Grossman, V.Bulović, M.G.Bawendi. *ACS Nano*, **10**, 3382 (2016)
116. S.A.Pawar, J.P.Jeong, D.S.Patil, V.M.More, R.S.Lee, J.C.Shin, W.J.Choi. *J. Korean Phys. Soc.*, **72**, 1188 (2018)
117. Q.Wu, H.Zhao, F.Huang, J.Hou, H.Cao, Z.Liu, S.Peng, G.Cao. *J. Phys. Chem. C*, **121**, 18430 (2017)
118. C.M.Evans, L.C.Cass, K.E.Knowles, D.B.Tice, R.P.H.Chang, E.A.Weiss. *J. Coord. Chem.*, **65**, 2391 (2012)
119. Y.Pu, F.Cai, D.Wang, J.-X.Wang, J.-F.Chen. *Ind. Eng. Chem. Res.*, **57**, 1790 (2018)
120. F.W.Low, C.W.Lai, S.B.Abd Hamid. *Ceram. Int.*, **43**, 625 (2017)
121. D.Chen, H.Feng, J.Li. *Chem. Rev.*, **112**, 6027 (2012)
122. J.Liu, Y.Xue, Y.Gao, D.Yu, M.Durstock, L.Dai. *Adv. Mater.*, **24**, 2228 (2012)
123. H.B.Yang, Y.Q.Dong, X.Wang, S.Y.Khoo, B.Liu. *ACS Appl. Mater. Interfaces*, **6**, 1092 (2014)
124. K.D.G.I.Jayawardena, R.Rhodes, K.K.Gandhi, M.R.Ranga Prabhath, G.D.M.R.Dabera, M.J.Beliatis, L.J.Rozanski, S.J.Henley, S.R.P.Silva. *J. Mater. Chem., A*, **1**, 9922 (2013)
125. A.Hu, Q.Wang, L.Chen, X.Hu, Y.Zhang, Y.Wu, Y.Chen. *ACS Appl. Mater. Interfaces*, **7**, 16078 (2015)
126. S.Qu, M.Li, L.Xie, X.Huang, J.Yang, N.Wang, S.Yang. *ACS Nano*, **7**, 4070 (2013)
127. S.-S.Li, K.-H.Tu, C.-C.Lin, C.-W.Chen, M.Chhowalla. *ACS Nano*, **4**, 3169 (2010)
128. J.-Y.-Jeon, J.-M.Yun, D.-Y.Kim, S.-I.Na, S.-S.Kim. *Sol. Energy Mater. Sol. Cells*, **105**, 96 (2012)
129. I.P.Murray, S.J.Lou, L.J.Cote, S.Loser, C.J.Kadleck, T.Xu, J.M.Szarko, B.S.Rolczynski, J.E.Johns, J.Huang, L.Yu, L.X.Chen, T.J.Marks, M.C.Hersam. *J. Phys. Chem. Lett.*, **2**, 3006 (2011)
130. K.Yuan, L.Chen, Y.Chen. *ACS Appl. Mater. Interfaces*, **6**, 21069 (2014)
131. E.Stratakis, M.M.Stylianakis, E.Koudoumas, E.Kymakis. *Nanoscale*, **5**, 4144 (2013)
132. J.Liu, Y.Xue, L.Dai. *J. Phys. Chem. Lett.*, **3**, 1928 (2012)
133. S.-H.Kim, C.-H.Lee, J.-M.Yun, Y.-J.Noh, S.-S.Kim, S.Lee, S.M.Jo, H.-I.Joh, S.-I.Na. *Nanoscale*, **6**, 7183 (2014)
134. C.Li, X.Yang, Y.Zhao, P.Zhang, Y.Tu, Y.Li. *Org. Electron.*, **15**, 2868 (2014)
135. E.-S.Choi, Y.-J.Jeon, S.-S.Kim, T.-W.Kim, Y.-J.Noh, S.-N.Kwon, S.-I.Na. *Appl. Phys. Lett.*, **107**, 023301 (2015)
136. E.Stratakis, K.Savva, D.Konios, C.Petridis, E.Kymakis. *Nanoscale*, **6**, 6925 (2014)
137. F.-C.Tang, F.-C.Wu, C.-T.Yen, J.Chang, W.-Y.Chou, S.-H.G.Chang, H.-L.Cheng. *Nanoscale*, **7**, 104 (2015)
138. B. R.Sutherland. *Joule*, **2**, 21 (2018)
139. C.Ding, Y.Zhang, F.Liu, Y.Kitabatake, S.Hayase, T.Toyoda, R.Wang, K.Yoshino, T.Minemoto, Q.Shen. *Nanoscale Horiz.*, **3**, 417 (2018)
140. Y.Cho, B.Hou, J.Lim, S.Lee, S.Pak, J.Hong, P.Giraud, A.R.Jang, Y.-W.Lee, J.Lee, J.E.Jang, H.J.Snaith, S.M.Morris, J.I.Sohn, S.Cha, J.M.Kim. *ACS Energy Lett.*, **3**, 1036 (2018)
141. L.Zhang, Z.C.Ding, T.Tong, J.Liu. *Nanoscale*, **9**, 3524 (2017)
142. J.-S.Ahn, J.-W.Ahn, Y.-C.Park, S.-J.Kim, E.-M.Han. *Mol. Cryst. Liq. Cryst.*, **654**, 22 (2017)
143. A.Yadav, A.Upadhyaya, S.K.Gupta, A.S.Verma, C.M.Singh Negi. *Superlatt. Microstruct.*, **120**, 788 (2018)
144. J.Li, J.Liu, C.Gao, G.Chen. *Int. J. Photoenergy*, **2011**, Article ID 392832 (2011)
145. J.Gao, C.L.Perkins, J.M.Luther, M.C.Hanna, H.-Y.Chen, O.E.Semonin, A.J.Nozik, R.J.Ellingson, M.C.Beard. *Nano Lett.*, **11**, 3263 (2011)
146. T.A.Amollo, G.T.Mola, V.O.Nyamori. *J. Mater. Sci.: Mater. Electron.*, **29**, 7820 (2018)
147. J.Liu, G.-H.Kim, Y.Xue, J.Y.Kim, J.-B.Baek, M.Durstock, L.Dai. *Adv. Mater.*, **26**, 786 (2014)
148. H.Park, S.Chang, M.Smith, S.Gradečak, J.Kong. *Sci. Rep.*, **3**, 1581 (2013)
149. S.Yang, Y.Hou, J.Xing, B.Zhang, F.Tian, X.H.Yang, H.G.Yang. *Chem. – Eur. J.*, **19**, 9366 (2013)
150. K.Yan, Z.Wei, J.Li, H.Chen, Y.Yi, X.Zheng, X.Long, Z.Wang, J.Wang, J.Xu, S.Yang. *Small*, **11**, 2269 (2015)
151. A.Klein, C.Körber, A.Wachau, F.Säuberlich, Y.Gassenbauer, R.Schafranek, S.P.Harvey, T.O.Mason. *Thin Solid Films*, **518**, 1197 (2009)
152. J.Meiss, C.L.Uhrich, K.Fehse, S.Pfuetzner, M.K.Riede, K.Leo. In *Photonics for Solar Energy Systems II. (Ser. Proceedings of SPIE.* Vol. 7002). (Bellingham, WA: SPIE — the International Society for Optical Engineering, 2008). No. 700210
153. L.F.Zagonel, M.Bäurer, A.Bailly, O.Renault, M.Hoffmann, S.J.Shih, D.Cockayne, N.J.Barrett. *J. Phys.: Condens. Matter*, **21**, 314013 (2009)
154. Q.Jiang, X.Sheng, B.Shi, X.Feng, T.Xu. *J. Phys. Chem. C*, **118**, 25878 (2014)

155. C.Tozlu, A.Mutlu, M.Can, A.K.Havare, S.Demic, S.Icli. *Appl. Surf. Sci.*, **422**, 1129 (2017)
156. D.Gu, S.K.Dey, P.Majhi. *Appl. Phys. Lett.*, **89**, 082907 (2006)
157. M.Wei, C.-F.Li, X.-R.Deng, H.Deng. *Energy Proc., Part A*, **16**, 76 (2012)
158. G.Zhao, W.Wang, T.-S.Bae, S.-G.Lee, C.Mun, S.Lee, H.Yu, G.-H.Lee, M.Song, J.Yun. *Nat. Commun.*, **6**, 8830 (2015)
159. H.Park, P.R.Brown, V.Bulović, J.Kong. *Nano Lett.*, **12**, 133 (2012)
160. H.Park, R.M.Howden, M.C.Barr, V.Bulović, K.Gleason, J.Kong. *ACS Nano*, **6**, 6370 (2012)
161. F.J.Lim, K.Ananthanarayanan, J.Luther, G.W.Ho. *J. Mater. Chem.*, **22**, 25057 (2012)
162. L.Kavan, P.Liska, S.M.Zakeeruddin, M.Grätzel. *ACS Appl. Mater. Interfaces*, **6**, 22343 (2014)
163. E.Ramasamy, W.J.Lee, D.Y.Lee, J.S.Song. *Electrochem. Commun.*, **10**, 1087 (2008)
164. L.Kavan, J.H.Yum, M.Grätzel. *ACS Nano*, **5**, 165 (2011)
165. Z.Liu, P.You, C.Xie, G.Tang, F.Yan. *Nano Energy*, **28**, 151 (2016)
166. L.Yin, K.Zhang, H.Luo, G.Cheng, X.Ma, Z.Xiong, X.Xiao. *Nanoscale*, **6**, 10879 (2014)
167. C.Liu, A.Wei, J.Liu, J.Lin. In *The 16th IEEE International Symposium on the Physical and Failure Analysis of Integrated Circuits. IEEE, Suzhou, Jiangsu, 2009*. P. 596
168. M.-E.Yeoh, K.-Y.Chan. *Int. J. Energy Res.*, **41**, 2446 (2017)
169. N.Baig, T. A.Saleh. *Mikrochim. Acta*, **185**, 283 (2018)
170. D.H.Shin, C.W.Jang, H.S.Lee, S.W.Seo, S.-H.Choi. *ACS Appl. Mater. Interfaces*, **10**, 3596 (2018)
171. N.V.Le, H.T.Nguyen, H.V.Le, T.T.P.Nguyen. *J. Electron. Mater.*, **46**, 274 (2017)
172. S.Sfaelou, V.Dracopoulos, P.Lianos. *J. Adv. Oxidation Technol.*, **17**, 53 (2014)
173. H.Park, S.Chang, J.Jean, J.J.Cheng, P.T.Araujo, M.Wang, M.G.Bawendi, M.S.Dresselhaus, V.Bulović, J.Kong, S.Gradečak. *Nano Lett.*, **13**, 233 (2013)